ISSN 2229-5518

Potentiodynamic Polarization, Electrochemical Impedance Spectroscopy (EIS) and Density Functional Theory Studies of Sulfa Guanidine Azomethine as Efficient Corrosion Inhibitors for Nickel Surface in Hydrochloric Acid Solution

Hala.M.Hassan[1], A.Attia[2], Wael A. Zordok[3] and A.M. Eldesoky[4]*

1Textile Technology Department, Industrial Education College,Beni-Suef University, Egypt and Chemistry Department, Faculty of Science, Jazan University, KSA.
2Department of Chemistry ,Faculty of Science,Mansoura University, Mansoura ,Egypt and Faculty of Science and Arts in Balgarn , Chemistry Department, King Khalid University, KSA.
3Department of Chemistry ,Faculty of Science,Zagazig University,Zagazig,Egypt and Department of Chemistry University College of Quanfudha, Umm Al -Qura University, KSA.
4*Engineering Chemistry Department, High Institute of Engineering &Technolog(New Damietta), Egypt and Al-Qunfudah Center for Scientific Research (QCSR), Al-Qunfudah University College, Umm Al-Qura University ,KSA.

Abstract- The corrosion inhibition properties of a new class of sulfa guanidine azomethine derivatives, namely sulfa guanidine azomethine 2,4 dihydroxy benzaldehyde and sulfa guanidine azomethine salisaldehyde for nickel corrosion in 0.1 M HCl medium were analysed by electrochemical impedance spectroscopy (EIS). An adequate structural model of the interface was usedand the values of the corresponding parameters were calculated and discussed. The experimental results showed that these compounds are excellent inhibitors for the nickel corrosion in acid solution and that the protection efficiency increased with increasing the inhibitors concentration. Electrochemical impedance data demonstrate that the addition of the sulfa guanidine azomethine derivatives in the corrosive solution decreases the charge capacitance and simultaneously increases the function of the charge/discharge of the interface, facilitating the formation of an adsorbed layer over the nickel surface. Adsorption of these inhibitors on the nickel surface obeys to the Frumkin adsorption isotherm. Thermodynamic adsorption parameters (K_{ads}, $\Delta G°_{ads}$) of investigated inhibitors were calculated from the linear form of Frumkin adsorption isotherm. Activation parameters of the corrosion process were calculated and discussed.Quantum chemical calculations using the Density Functional Theory (DFT) were performed on sulfa guanidine azomethine derivatives to determine the relationship between molecular structure and their inhibition efficiencies. The results of the quantum chemical calculations and experimental inhibition efficiency were subjected to correlation analysis and indicate that their inhibition effect is closely related to EHOMO, ELUMO, and the energy difference (ΔE).

Keywords: DFT Theory, Sulfa Guanidine Azomethine, Efficient Inhibitors, Nickel.

*Correspondence Author: E-mail: E-mail: a.m.eldesoky@hotmail.com

1. INTRODUCTION

Nickel is one of the most important metals and it used in a large number of applications. The pure nickel has a good corrosion resistance. Nickel is used as alloying element with other metals. Also, nickel plays an important role in repair or replacement of the diseased bone tissue. The corrosion resistance of nickel is due to the formation of a passive film on its surface upon exposure to the corrosive media. Nevertheless, nickel could be attacked by acidic media in a considerable rate. Acid solutions are commonly used in chemical industry to remove mill scales from metallic surface and because nickel is frequently used in contact with acidic solutions, its corrosion rate must be controlled. One of the useful methods of controlling the corrosion process is the addition of inhibitors. The use of inhibitors is one of the most practical methods for protection against metallic corrosion, especially in acidic media [1]. The action of inhibition of nickel and its alloys in acidic media by various organic and inorganic inhibitors has been widely studied [2-28]. In general, organic inhibitors such as amines, acetylenic alcohols, heterocyclic compounds, natural rosemary oil, β-aminoketone derivatives, halides, tween surfactants and some phosphonium inhibitors have found use as inhibitors in industrial applications [29- 35].

ISSN 2229-5518

The present work was designed to study the corrosion inhibition of nickel in 0.1 M HCl solution by some sulfa guanidine azomethine derivatives using electrochemical techniques. The density function theory (DFT) is used to study the structural properties of two sulfa guanidine azomethine derivatives in aqueous phase in an attempt to understand their inhibition mechanism. The protection efficiencies of these compounds showed a certain relationship to the highest occupied molecular orbital (EHOMO) and the lowest unoccupied molecular orbital (ELUMO), the energy difference (ΔE) between EHOMO and ELUMO.

The names, chemical and molecular structures of the investigated derivatives are shown in Table (1) [36].

Table (1): The names, chemical and molecular structures of the investigated derivatives

Cpd. No.	Name	Structure	Molecular Weight& Chemical Formula
(A)	Sulfa Guanidine Azomethine 2,4 Dihydroxy Benzaldehyde	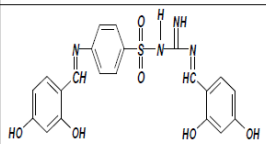	454.0, $C_{21}H_{18}N_4O_6S$
(B)	Sulfa Guanidine Azomethine Salisaldehyde	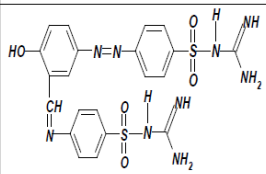	511.0, $C_{21}H_{21}N_9O_5S$

2. Computational details

Density functional theory (DFT) was used to compute of the effect some sulfa compounds on the degree of inhibition for the corrosion rate theoretically and detect the exact structure of these compounds also show the stable compound which can be used as inhibitor more than others. The effect of substitution was investigated theoretically and the excited state for all compounds was investigated by applying UV calculations to determine the different types of electronic transition which can be occurred on these compounds with different substituent. The Frontier molecular orbitals were studied for its important role in the electric and optical properties, as well as in UV-Vis. Spectra and chemical reactions. Such computational characterization reduces time consuming experiments for biomedical and pharmaceutical studies of the drugs and its complexes. Profiles of the optimal set and geometry of these complexes were simulated by applying the GAUSSIAN 98W package of programs [37] at B3LYP/Cep-31G [38] level of theory.

3. Experimental details

3.1. Materials and chemicals

The corrosion tests were performed on nickel rods with a composition (in wt. %): Fe 0.05; Al 0.005; Co 0.005; Mn 0.005, Ti 0.05 and nickel balance. These rods were mounted in Teflon. An epoxy resin was used to fill the space between Teflon and Ni electrode. Rods with an exposed length of 1 cm (φ = 1.25 mm) were used for all electrochemical measurements. Prior to experiments, all of the electrodes were gradually abraded with different grit emery papers up to 4/0 grit size in order to obtain a smooth surface, degreased with acetone, washing with bidistilled water and finally dried with cool air and stored in a vacuum desiccators.

The aggressive solutions, 0.1 M HCl were prepared by dilution of analytical grade 37 % HCl with bidistilled water. The investigated inhibitors were purchased from SIGMA-ALDRICH and used as received.

Stock solutions (1 x 10^{-3} M) were made in ethanol to ensure solubility. These stock solutions were used for all experimental purposes. Table 1 shows the molecular structure of investigated inhibitors.

3.2 Electrochemical techniques

Before starting the experiments, the working electrodes were immersed in the test solution for 30 min until a steady potential reached, then the electrochemical measurements were carried out in a conventional three electrodes cylindrical glass cell with a capacity of 100 ml. Saturated calomel (SCE) and a platinum foil were used as reference and auxiliary electrodes, respectively. The reference electrode was connected to a Luggin capillary to minimize IR drop. The polarization curves were obtained potentiodynamically in potential range - 800 mV to + 800 mV versus open circuit potential (EOC) with the scan rate 5 mV s^{-1}.

The inhibition efficiencies (%IE) and surface coverage (θ) were calculated from the following equation [39]:

$$\% IE = \theta \times 100 = [1- (i_{corr}(inh) / i_{corr} (free)] \times 100 \quad (1)$$

Where (i_{corr} (free)) and (i_{corr} (inh)) are the corrosion current densities in the absence and presence of inhibitor, respectively.

Impedance measurements were carried out using Ac signal with amplitude of 5 mV at open circuit potential (OCP) in the frequency range from 100 kHz to 0.5 Hz. The impedance data were fitted to most appropriate equivalent circuit. The impedance parameters were obtained from Nyquist plots. The double layer capacitance (Cdl) values were calculated from the frequency at which the imaginary component of impedance was maximum (-Zimg, max) using the following relation:

Cdl = (1/2πfmax Rct) **(2)**

% IE was calculated using the following equation:

% IE = [1 – [1- (Roct / Rct)] x 100 **(3)**

Where R_{oct} & R_{ct} refer to charge transfer resistance without and with the addition of the inhibitor, respectively.

All experiments were conducted at 30 ± °C. Measurements were performed using Gamry PCI 300/4 Instrument Potentiostat/Galvanostat/ZRA. This includes Gamry Framework system based on the ESA400, Gamry applications that include DC105 for dc corrosion measurements and EIS300 for electrochemical impedance spectroscopy along with a computer for collecting data. Echem Analyst 5.21 software was used for plotting, graphing and fitting data. All the potentials reported are referred to SCE.

4. Results and Discussion

4.1. Theoretical (Computational) Study

The geometric parameters and energies were computed by density functional theory at the B3LYP/Cep-31G level of theory, using the GAUSSIAN 98W package of the programs, on geometries that were optimized at Cep-31G basis set. The high basis set was chosen to detect the energies at a highly accurate level. The atomic charges were computed using the natural atomic orbital populations. The B3LYP is the keyword for the hybrid functional [40], which is a linear combination of the gradient functionals proposed by Becke [41] and Lee, Yang and Parr [42], together with the Hartree-Fock local exchange function [43].

4.1.1 Structural Parameters and Model of Sulfa Compounds

A- Sulfa Guanidine Azomethine 2,4 Dihydroxy Benzaldehyde

The activity of sulfa compounds is mainly determined by its fine structure, the sulfa azomethine 2,4 dihydroxy benzaldehyde has many characteristic structural features. The molecule is a highly sterically-hindered, there are three aromatic rings. The molecule is non planer, there are two plans one occupied by central aromatic ring and other plane occupied by the two terminal aromatic rings and also, the two plans are perpendicular respect to each other. The bond length N1-C2 is 1.346 Å, N1-C3 is 1.347 Å , also the N28-C29 is 1.347 Å there is a double bond characters C and N atoms [44], whereas C2-N15 is double bond 1.287Å. Detailed analysis of corresponding bond lengths in various sulfa molecules was given elsewhere [45]. All distances and angles between the atoms of the sulfa compound system are given in Table (2). The S19-O20 and S19-O21 bond lengths are 1.440 Å and 1.439 Å respectively, the C36-O37 and C34-O39 bond lengths are 1.355 Å and 1.359 Å respectively, also the C8-O11 and C10-O13 bond lengths are 1.360 Å and 1.363 Å respectively.

The molecule is a highly sterically-hindered, the sulfa guanidine azomethine 2,4 dihydroxy benzaldehyde compound occupied two plans they are perpendicular to each other. The two terminal aromatic rings are out of plane of central aromatic ring the dihedral angle N17S19C22C23, -114.17° and C29N28C25C24, 117.38°, so the two terminal aromatic rings are axially oriented from the central aromatic ring. Also the terminal phenyl ring lying out of plane of the molecule. This observation is supported by the values of calculated dihedral angles: C29N28C25C26,-64.68°, and N17S19C22C27, 65.66°, where the values are neither zero nor 180°. Fig. (1), shows the optimized geometrical structure of sulfa guanidine azomethine 2,4 dihydroxy benzaldehyde compound, the dihedral angles C2N17S19C22 is 25.89° and N28C29C31C32 is 178.68° also, N28C29C31C36, -1.63° ≈ 0.00° and C2N17S19O20 is 132.67° which confirms that the S19 and N28 lying out of the plane occupied by the two terminal aromatic rings and lying in the same plane of the central aromatic ring. The dihedral angles C25N28C29C31 is -18.45° and C2N17S19C21 is -84.78° also, C3N1C2N17, 34.45° and C2N1C3C4 is -176.79° which confirms that The C25N28 bond lying in the same plane of C24S19 bond and the phenyl ring is not lying in the same plane of the central aromatic ring.

Table (2) gives the optimized geometry of sulfa guanidine azomethine 2,4 dihydroxy benzaldehyde as obtained from B3LYP/Cep-31G calculations. These data are drowning to give the optimized geometry of molecule. The value of bond angle N1C3C4 is 122.27°, C2N1C3 is 121.16°, N1C2N15 is 116.76°, N28C29C31 is 135.98°, C25N28C29 is 125.60° and N15C2N17 is 117.35° reflects on sp2 hybridization of these central atoms. The values of bond distances are compared nicely with that obtained from X-ray data. Comparisons of the performance of different DFT methods allow outlining the main trends of these theoretical approaches which are necessary to better understand the properties and reaction mechanisms of sulfa guanidine azomethine 2,4 dihydroxy benzaldehyde compound. However, till now, no attempt has been made to analyze the application of various DFT methods and different basis sets for accurate calculations of structure of sulfa guanidine azomethine 2,4 dihydroxy benzaldehyde [46-49].

The S atom is bonded strongly with surrounded two oxygen atoms, nitrogen and carbon Also the charge

accumulated on S19 (1.222), O20 (-0.602) and O21 (-0.616). The charge accumulated in N1 (-0.298), N28 (-0.229) and N15 (-0.452), N17 (-0.442). The presence of four -OH groups on the two terminal aromatic rings effect on the charge spreading overall sulfa compound, the charge on O11 (-0.344), O13 (-0.349), C8 (0.285), C10 (0.273) and O37 (-0.352), O39 (-0.331), C34 (0.227), C36 (0.218). The energy of this compound is -301.933439965 au and very lower value of dipole 2.53D.

B- Sulfa Guanidine Azomethine Salisaldehyde

The molecule is non planer, there are two plans one occupied by two terminal ends and other plane occupied by two aromatic rings around azo group and also, the two plans are perpendicular respect to each other. The bond length N1-C2 is 1.339 Å, C2-N3 is 1.286 Å , there is a double bond characters C and N atoms, whereas N18-N19 is double bond 1.248Å. All distances and angles between the atoms of the sulfa compound system are given in Table (3). The S9-O10 and S9-O11 bond lengths of SO2 at the 1st terminal end are 1.438 and 1.439 Å and the S37-O38 and S37-O39 bond lengths of SO2 at the 2nd terminal end of sulfa molecule are 1.438 and 1.439 Å, the C28-N30 bond length is 1.347 Å and the bond length C42-N43 is 1.286 with double bond character.

The molecule is a highly sterically-hindered, the Sulfa guanidine azomethine salisaldehyde compound occupied two plans they are perpendicular to each other. This result can be confirmed from the values of the dihedral angle C28N30C31C36, 81.27° and C28N30C31C32, -97.52°, where the values are neither zero nor 180°, so the terminal end of aromatic ring is axially oriented from the ring and then out of plane occupied by other two aromatic rings around azo group. Also the two aromatic rings around the azo group lying in the same plane. This observation is supported by the values of calculated dihedral angles: N19N18C15C16, -0.52° ≈ 0.00, and N19N18C15C14, 179.49°, C15N18N19C20 is -178.29°. Fig. (2), shows the optimized geometrical structure of Sulfa guanidine azomethine salisaldehyde compound.

Table (3) gives the optimized geometry of sulfa guanidine azomethine salisaldehyde as obtained from B3LYP/Cep-31G calculations. These data are drowning to give the optimized geometry of molecule. The value of bond angle N1C2N3 is 118.56°, C24C28N30 is 124.02°, N40C42N45 is 122.17° and N1C2N5 is 122.54° and C28N30C31 is 116.86° reflects on sp2 hybridization of N30, the same result is obtained with C2. The bond angles O38S37O39 is 124.39°, C15N18N19 is 117.89° and N18N19C20 is 118.59° these results confirmed that the azo group not linear as seen in Fig. (2).

The S atom is bonded strongly with surrounded two oxygen atoms, nitrogen and carbon atom, Also the charge accumulated on S9 (1.209), O10 (-0.600), and O11 (-0.601) for the 1st terminal end, S37 (1.222), O38 (-0.593) and O39 (-0.604) for the 2nd terminal end. The charge accumulated in N5 (-0.429) and N40 (-0.418) also the charge accumulated on two nitrogen atoms of azo group N18 is (-0.085) and N19 is (-0.069). The charge on C28 (0.114), N30 (-0.253). There is only one -OH group at the central aromatic ring which effect on the charge spreading overall sulfa compound, the charge on O26 (-0.361), C23 (0.218). The energy of this compound is -350.016798386 au and not highly dipole 6.663D which result from the presence of OH group. This sulfa compound is more stable than other because of it has more negative value of energy and also it has posses higher value of dipole moment which reflects that the charge spread over all molecule.

4.1.2. Frontier Molecular Orbitals

The frontier molecular orbitals play also an important role in the electric and optical properties, as well as in UV-Vis. Spectra and chemical reactions [50]. Fig. 3 shows the distributions and energy levels of HOMO and LUMO orbitals computed for the all sulfa compounds. For sulfa guanidine azomethine 2,4 dihydroxy benzaldehyde compound the values of the energy of HOMO and LUMO are given in Table (3), the difference between HOMO and LUMO is 0.10367 and for sulfa guanidine azomethine salisaldehyde compound the values of HOMO and LUMO are given in Table (4), the difference between HOMO and LUMO is 0.06504, also the values of HOMO-1 , HOMO-2, LUMO+1 and LUMO+2 are given in Table (4)

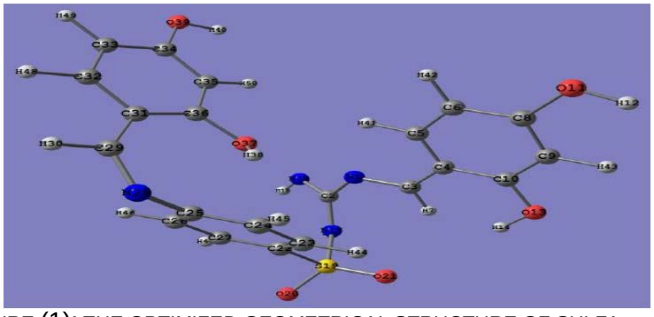

FIGURE (1): THE OPTIMIZED GEOMETRICAL STRUCTURE OF SULFA GUANIDINE AZOMETHINE 2,4 DIHYDROXY BENZALDEHYDE COMPOUND BY USING B3LYP/CEP-31G

ISSN 2229-5518

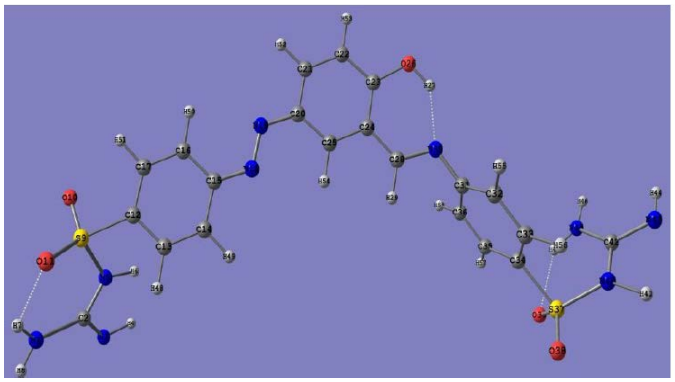

FIGURE (2): OPTIMIZED GEOMETRICAL STRUCTURE OF SULFA GUANIDINE AZOMETHINE SALISALDEHYDE COMPOUND BY USING B3LYP/CEP-31G

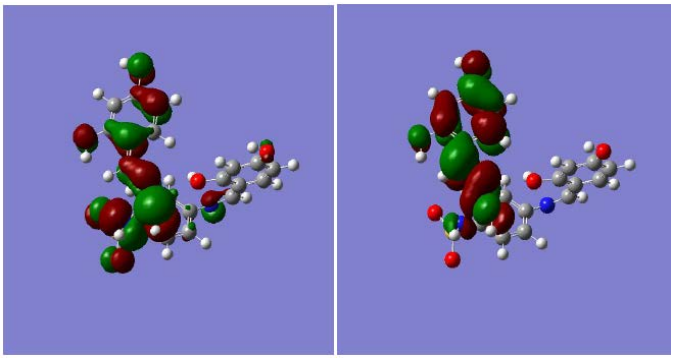

SULFA GUANIDINE AZOMETHINE 2,4 DIHYDROXY BENZALDEH

HOMO LUMO

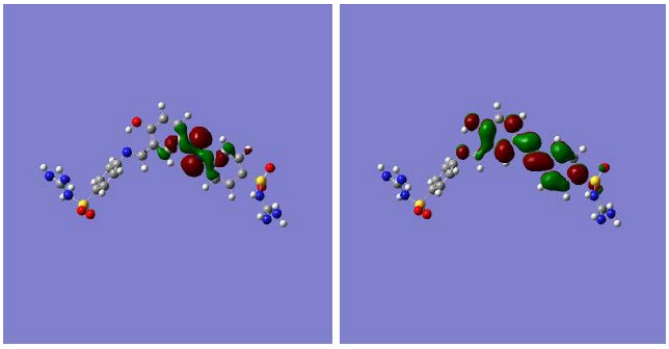

SULFA GUANIDINE AZOMETHINE SALISALDEHYDE

HOMO LUMO

FIGURE (3): MOLECULAR ORBITAL SURFACES AND ENERGY LEVELS OF SULFA GUANIDINE AZOMETHINE 2,4 DIHYDROXY BENZALDEHYDE AND SULFA GUANIDINE AZOMETHINE SALISALDEHYDE COMPOUND BY USING B3LYP/CEP-31G

TABLE (2): EQUILIBRIUM GEOMETRIC PARAMETERS BOND LENGTHS (Å), BOND ANGLES (˚), DIHEDRAL ANGLES (˚) AND CHARGE DENSITY OF SULFA GUANIDINE AZOMETHINE 2,4 DIHYDROXY BENZALDEHYDE COMPOUND BY USING DFT/B3LYP/CEP-31G.

							Bond length (Å)
N1-C2	1.346	C4-C10	1.351	S19-O20	1.440	C25-N28	1.345
N1-C3	1.347	C10-O13	1.363	S19-C22	1.743	N28-C29	1.347
C3-C4	1.346	C8-O11	1.360	C22-C23	1.347	C29-C31	1.349
C5-C6	1.341	C2-N15	1.287	C23-C24	1.342	C31-C32	1.351
C6-C8	1.341	C2-N17	1.347	C25-C26	1.342	C32-C33	1.341
C8-C9	1.343	N17-S19	1.638	C26-C27	1.342	C36-O37	1.355
C9-C10	1.345	S19-O21	1.439	C22-C27	1.347	C34-O39	1.359
							Bond angle (˚)
N1C3C4	122.27	C5C4C10	118.71	N1C2N15	116.76	O20S19O21	123.11
C3C4C5	120.48	C6C8O11	121.13	N1C2N17	125.89	O21S19C22	103.80
C3C4C10	120.82	C9C8O11	121.71	N15C2N17	117.35	O20S19C22	100.66
C4C10C9	118.89	C4C10O13	122.98	C2N17S19	126.56	S19C22C23	121.79
C8C9C10	123.31	C9C10O13	118.39	N17S19C22	102.29	S19C22C27	119.77
C6C8C9	117.17	C2N1C3	121.16	N17S19O21	112.27	C24C25N28	119.25
C5C6C8	120.82	N28C29C31	135.98	N17S19O20	111.35	C26C25N28	120.91
C4C5C6	121.40	C35C34O39	121.88	C31C36O37	123.69	C25N28C29	125.60
						C35C36O37	116.71
							Dihedral angles (˚)
C2N1C3C4	-176.79	C3N1C2N17	34.45	C2N17S19C22	25.89		
C2N17S19O20	132.67	C2N17S19O21	-84.78	N17S19C22C23	-114.17		
N17S19C22C27	65.66	C25N28C29C31	-18.45	C29N28C25C26	-64.68		
C29N28C25C24	117.38	N28C29C31C32	178.68	N28C29C31C36	-1.63		

							Charges
N1	-0.298	C10	0.273	C22	-0.09	C31	0.014
C2	0.438	O11	-0.344	C23	0.026	C32	-0.044
C3	0.156	O13	-0.349	C24	-0.105	C33	-0.074
C4	-0.073	N15	-0.452	C25	0.227	C34	0.227
C5	0.034	N17	-0.442	C26	-0.077	C35	-0.165
C6	-0.129	S19	1.222	C27	0.028	C36	0.218
C8	0.285	O20	-0.602	N28	-0.229	O37	-0.352
C9	-0.19	O21	-0.616	C29	0.004	O39	-0.331
			Total energy/au				-301.933439965
			Total dipole moment/D				2.53

TABLE (3): EQUILIBRIUM GEOMETRIC PARAMETERS BOND LENGTHS (Å), BOND ANGLES (˚), DIHEDRAL ANGLES (˚) AND CHARGE DENSITY OF SULFA GUANIDINE AZOMETHINE SALISALDEHYDE COMPOUND BY USING DFT/B3LYP/CEP-31G.

							Bond length (Å)
N1-C2	1.339	C12-C13	1.346	N18-N19	1.248	C24-C28	1.347
C2-N3	1.286	C13-C14	1.342	N18-C20	1.265	C28-N30	1.348
C2-N5	1.345	C14-C15	1.345	N40-C42	1.345	N30-C31	1.348
N5-S9	1.636	C15-C16	1.346	N43-C42	1.286	C34-S37	1.745
S9-O10	1.438	C16-C17	1.343	C42-N45	1.339	S37-O39	1.438
S9-O11	1.439	C12-C17	1.345	C23-C24	1.351	S37-O38	1.439
S9-C12	1.745	C15-N18	1.266	C24-C25	1.349	S37-N40	1.636
							Bond angle (˚)
N1C2N3	118.56	S9C12C17	121.82	C24C23O26	124.19	C34S37O39	103.41
N1C2N5	122.54	C16C15N18	125.52	C24C28N30	124.02	C34S37O38	100.29
N3C2N5	118.89	C14C15N18	116.55	C28N30C31	116.86	O38S37O39	124.39
C2N5S9	125.06	C15N18N19	117.75	N30C31C32	119.61	O38S37N40	111.82
N5S9C12	99.69	N18N19C20	118.59	N30C31C36	120.49	O39S37N40	112.49
N5S9O10	112.01	N19C20C21	116.13	C33C34S37	119.71	S37N40C42	125.55
N5S9O11	112.99	N19C20C25	125.98	C35C34S37	121.94	N40C42N43	118.75
S9C12C13	120.29	C22C23O26	117.58	C34S37N40	99.91	N40C42N45	122.17
							Dihedral angles (˚)
N43C42N40S37	175.97	S37N40C42N45	-2.26	N30C28C24C25	179.34		
C42N40S37C34	-63.94	C42N40S37O39	45.16	C15N18N19C20	-178.29		
C42N40S37O38	-169.32	N40S37C34C33	-56.97	N19N18C15C16	-0.52		
N40S37C34C35	122.19	C28N30C31C32	-97.52	N5S9C12C17	133.54		
C28N30C31C36	81.27	C24C28N30C31	179.48	N1C2N5S9	-6.33		
N19N18C15C14	179.49	N30C28C24C23	-0.50	C2N5S9O10	-104.04		
N5S9C12C13	-47.28	C2N5S9C12	148.21	C2N5S9O11	43.37		

							Charges
N1	-0.389	C14	-0.096	C23	0.218	C34	-0.089
C2	0.471	C15	0.197	C24	-0.011	C35	0.019
N3	-0.518	C16	-0.096	C25	-0.081	C36	-0.094
N5	-0.429	C17	0.025	O26	-0.361	S37	1.222
S9	1.209	N18	-0.085	C28	0.114	O38	-0.593
O10	-0.600	N19	-0.069	N30	-0.253	O39	-0.604
O11	-0.601	C20	0.158	C31	0.211	N40	-0.418
C12	-0.093	C21	-0.054	C32	-0.091	C42	0.468
C13	0.015	C22	-0.072	C33	0.02	N43	-0.524
						N45	-0.409
			Total energy/au				-350.016798386
			Total dipole moment/D				6.663

TABLE (4): VALUES OF ENERGY (EV) OF HOMO AND LUMO FOR (A) SULFA GUANIDINE AZOMETHINE 2,4 DIHYDROXY BENZALDEHYDE AND (B) SULFA GUANIDINE AZOMETHINE SALISALDEHYDE COMPOUND BY USING B3LYP/CEP-31G.

	(A)	(B)
$LUMO^{+2}$	-0.18462	-0.14772
$LUMO^{+1}$	-0.18956	-0.19184
LUMO	-0.19197	-0.21334
HOMO	-0.29564	-0.27838
$HOMO^{-1}$	-0.30557	-0.29653
$HOMO^{-2}$	-0.30678	-0.29685
ΔE= HOMO - LUMO	0.10367	0.06504

4.2. Potentiodynamic Polarization Measurements

Figure (4) shows typical polarization curves for nickel in 0.1 M HCl solution with and without different concentrations of inhibitor (A) at 30 °C. Similar curves were obtained for other derivative (not shown). Table (5) collect the associated corrosion electrochemical parameters, i.e. corrosion potential (E_{corr}), corrosion current density (i_{corr}) derived from polarization curves by extrapolation, anodic and cathodic Tafel slopes (β_a & β_c) the degree of surface coverage (θ), as well as the percentage inhibition efficiency (% IE).

It is seen that the addition of investigated sulfa guanidine azomethine derivatives shift both the cathodic and anodic branches of the polarization curves of the pure acid solution to lower values of current density indicating the inhibition of both the hydrogen evolution and nickel dissolution reactions. The corrosion potential is almost unchanged. These observations indicate that a mixed-type control and investigated sulfa guanidine azomethine derivatives are inhibitors of mixed-type for the corrosion of

nickel in 0.1 M HCl [51-53]. It is evident that by increasing the inhibitor concentration a decrease in corrosion current densities and an increase in % IE were observed, suggesting that the adsorption protective film tends to be more complete and stable on nickel surface. The anodic and cathodic Tafel slope values are different from the ones obtained with and without the presence of investigated sulfa guanidine azomethine derivatives, respectively, suggesting that the mechanism of the reaction of nickel in 0.1 M HCl is influenced by the presence of investigated inhibitors. The higher values of % IE indicate the higher surface coverage, due to the adsorption of inhibitors on the metal surface. The order of decreasing inhibition efficiency of the investigated sulfa guanidine azomethine derivatives is as follows: Compound (B) > Compound (A).

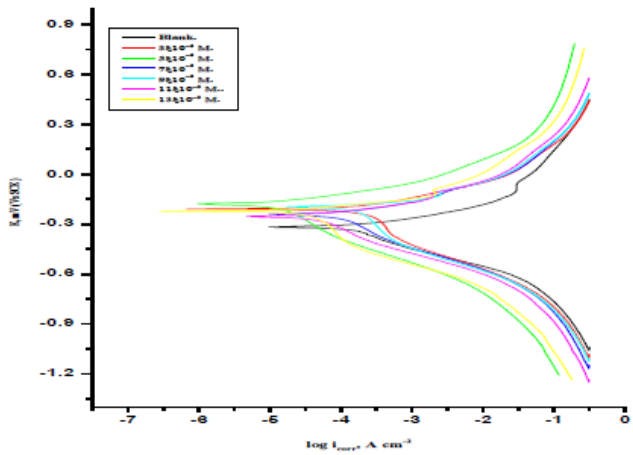

FIGURE (4): THE POTENTIODYNAMIC POLARIZATION CURVES FOR THE CORROSION OF NICKEL 0.1 M HCL IN ABSENCE AND PRESENCE OF DIFFERENT CONCENTRATIONS OF INHIBITOR (A) AT 30 °C.

TABLE (5): EFFECT OF CONCENTRATION OF THE INVESTIGATED SULFA GUANIDINE AZOMETHINE DERIVATIVES ON THE CORROSION POTENTIAL(E_{CORR}), CORROSION CURRENT DENSITY (I_{CORR}), TAFEL SLOPES (B_A, B_C), DEGREE OF SURFACE COVERAGE (Θ), AND INHIBITION EFFICIENCY (% IE) FOR THE CORROSION OF NICKEL IN 0.1 M HCL AT 30 °C.

Inh.	Conc, M	$-E_{corr.}$, mV vs SCE	$i_{corr.}$ x10⁴ A cm⁻²	β_a, mV dec⁻¹	β_c, mV dec⁻¹	θ	% IE
Blank	-----	321	4.55	259	244	----	-----
(A)	3 X 10⁻⁶	235	3.01	219	271	0.338	33.8
	5 X 10⁻⁶	177	2.50	234	259	0.450	45.0
	7 X 10⁻⁶	219	2.22	239	270	0.512	51.2
	9 X 10⁻⁶	134	1.90	201	286	0.582	58.2
	11 X 10⁻⁶	205	1.69	192	284	0.628	62.8
	13 X 10⁻⁶	323	1.61	292	288	0.646	64.6
(B)	3 X 10⁻⁶	257	2.79	246	291	0.386	38.6
	5 X 10⁻⁶	218	2.28	262	322	0.498	49.8
	7 X 10⁻⁶	301	2.27	223	269	0.501	50.1
	9 X 10⁻⁶	262	1.79	271	292	0.606	60.6
	11 X 10⁻⁶	211	1.72	251	277	0.621	62.1
	13 X 10⁻⁶	201	0.63	228	268	0.861	86.1

4.3. Electrochemical impedance spectroscopy (EIS)

The corrosion behavior of nickel in 0.1 M HCl solution in absence and presence of different concentrations of the investigated sulfa guanidine azomethine derivatives was investigated by the EIS method at 30 °C. Figure (5) shows the Nyquist plots for nickel in 0.1 M HCl solution in the absence and presence of different concentrations of the inhibitor (A) at 30 °C. Similar curves were obtained for other derivative (not shown). These plots having the shape of semicircle for all the concentrations of examined inhibitors indicate that the corrosion is mainly controlled by charge transfer process. The obtained Nyquist impedance diagrams in most cases doesn't show perfect semicircle, generally attributed to the frequency dispersion [54] as a result of roughness and in homogenates of the electrode surface. The data revealed that, each impedance diagram consists of a large capacitive loop with low frequencies dispersion (inductive arc) which is generally attributed to anodic adsorbed intermediates controlling the anodic process [55-57]. In 0.1 M HCl solution and in the presence of various concentrations of inhibitors, the impedance diagrams show the same trend (one capacitive loop), however, the diameter of this capacitive loop increases with increasing concentration, due to the increase in the number of adsorbed inhibitor molecules when the concentration was raised. From the analysis of Nyquist diagram, the main parameters are the charge transfer resistance R_{ct}, and the capacity of double layer C_{dl} which is defined as:

$$Cdl = 1/ (2\pi f_{max} R_{ct}) \quad (4)$$

The surface coverage (θ) and the inhibition efficiencies (% IE) are defined by the following equation:

$$\% IE = \theta \times 100 = [1- (R_{oct} / R_{ct})] \times 100 \quad (5)$$

Where f_{max} is the maximum frequency, R_{oct} & R_{ct} are the charge transfer resistances in the absence and presence of inhibitor, respectively. The associated parameters with the impedance diagrams are given in Table (6).

From the impedance results Table (6) we found that as the inhibitor concentration increased, R_{ct} values increased, but C_{dl} values tended to decrease. The decrease in C_{dl}, which can result from a decrease in local dielectric constant and/or an increase in the thickness of the electrical double layer, suggests that sulfa guanidine azomethine derivatives function by adsorption at the metal-solution interface [58]. The change in R_{ct} and C_{dl} values was caused by the gradual replacement of water molecules by the anions of Cl^- and adsorption of the organic molecules on the metal surface, reducing the extent of dissolution [59]. The order of inhibition efficiency obtained from EIS

measurements decreases as follows: Compound (B) > Compound (A). The % IE obtained from EIS measurements are close to those deduced from polarization measurements. The charge transfer resistance R_{ct} and the double layer capacitance C_{dl} values were derived by using the equivalent circuit, Figure (6).

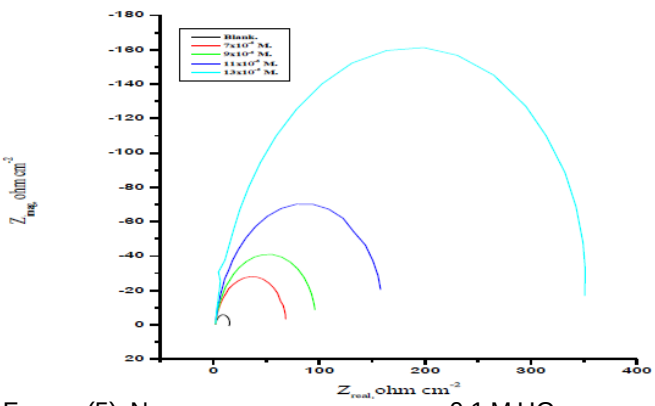

FIGURE (5): NYQUIST PLOTS FOR NICKEL IN 0.1 M HCL WITHOUT AND WITH VARIOUS CONCENTRATIONS OF INHIBITOR (A) AT 30 °C.

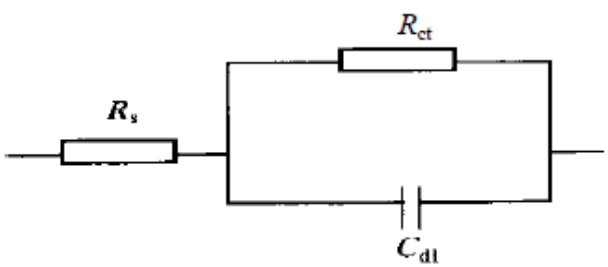

FIGURE (6): EQUIVALENT CIRCUIT MODEL USED IN THE FITTING OF THE IMPEDANCE DATA OF NICKEL

TABLE (6): ELECTROCHEMICAL KINETIC PARAMETERS OBTAINED BY EIS TECHNIQUE FOR NI IN 0.1 M HCL WITHOUT AND WITH VARIOUS CONCENTRATIONS OF SULFA GUANIDINE AZOMETHINE DERIVATIVES 30 °C.

Inhibitor	Conc., M	C_{dl} µF cm⁻²	R_{ct} Ohm cm²	θ	% IE
Blank	-------	16.4	12.7	------	-------
(A)	7x10⁻⁶	16.9	20.3	0.374	37.4
	9x10⁻⁶	12.4	24.7	0.485	48.5
	11x10⁻⁶	11.0	31.1	0.591	59.1
	13x10⁻⁶	10.9	38.4	0.669	66.9
(B)	7x10⁻⁶	14.5	22.7	0.440	44.0
	9x10⁻⁶	13.3	32.0	0.603	60.3
	11x10⁻⁶	10.4	37.6	0.662	66.2
	13x10⁻⁶	8.7	43.1	0.705	70.5

4.4. Adsorption isotherm

It is generally assumed that the adsorption of the inhibitors on the metal surface is the essential step in the inhibition mechanism [60]. To determine the adsorption mode, various isotherms were tested and the Frumkin mode should be the best. This Frumkin model has been used for other inhibitor systems [61, 62]. According to this isotherm θ is related to inhibitor concentration via:

$$[\theta / (1-\theta) \exp(-2a\theta) = KC] \quad (6)$$

Or its linear form:

$$\ln[[\theta / (1-\theta)C] = \ln K_{ads} + 2a\theta \quad (7)$$

Where a is the interaction parameter between molecules adsorbed on the metal surface and K_{ads} the equilibrium constant of adsorption. Figure (7) represents the linear relationship of the Frumkin adsorption isotherm. By plotting ln [[θ/(1-θ)C] vs. θ, straight lines were obtained for all investigated inhibitors. The equilibrium constant (K_{ads}) is related to the free energy of adsorption ($\Delta G°_{ads}$) by:

$$K_{ads} = (1/55.5) \exp(-\Delta G°_{ads}/RT) \quad (8)$$

Where 55.5 is the molar concentration of water in solution in mol L^{-1}. The slope of the linear fitting of Frumkin gave the values of (a) and the intercepts gave the values of K_{ads} for all the investigated inhibitors (Table 7). The negative values of (a) indicates the presence of repulsive forces between the adsorbed species of the investigated inhibitors and the increasing values of K_{ads} from compound (A) to compound (B) reflects the increasing capability, due to structural formation, on the metal surface [63]. The calculated $\Delta G°_{ads}$ values, using Eq.8, were also given in Table (7). The large negative values of $\Delta G°_{ads}$ ensure the spontaneity of the adsorption process and the stability of the adsorbed layer on Ni surface [64, 65] as well as a strong interaction between inhibitors molecules and the metal surface [66].

Generally, absolute values of $\Delta G°_{ads}$ up to 20 kJ mol^{-1} are consistent with physisorption, while those around 40 kJ mol^{-1} or higher are associated with chemisorptions as a result of the sharing or transfer of electrons from organic molecules to the metal surface to form a coordinate type of metal bond. Here the calculated values of $\Delta G°_{ads}$ are ranging from -45.1 and - 46.3 kJ mol^{-1}, indicating that the adsorption mechanism of the inhibitors on Ni surface in 0.1 M HCl solution at the studied temperatures is due to mixed type of adsorption (electrostatic-adsorption and chemisorptions) [67]. The decrease of % IE with rise in temperature indicates that the physisorption has the major contribution while the chemisorptions have the minor contribution in the inhibition mechanism [68].

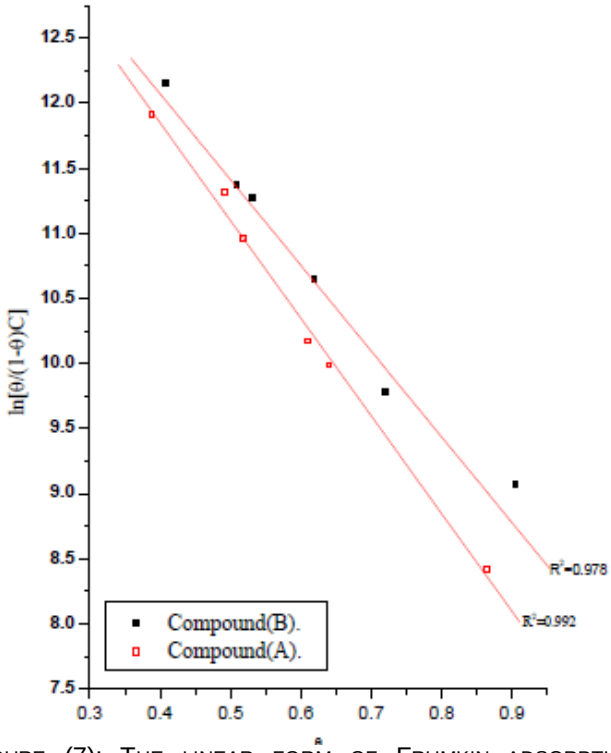

FIGURE (7): THE LINEAR FORM OF FRUMKIN ADSORPTION ISOTHERM OF INVESTIGATED INHIBITORS ON NICKEL SURFACE IN 0.1 M HCL SOLUTION AT 30 °C.

Table (7): Interaction parameters (a), adsorption equilibrium constant (K_{ads}) and free energy (ΔG°_{ads}) of nickel dissolution in 0.1 M HCl in the presence of investigated sulfa guanidine azomethine derivatives at 30 °C

Compounds	-a	K_{ads} x 10^{-6} M^{-1}	$-\Delta G^{\circ}_{ads}$, kJ mol^{-1}
(A)	6.4	2.4	45.1
(B)	3.9	3.8.0	46.3

4.5. Kinetic parameters

The influence of solution temperature on the inhibition performance of investigated inhibitors for nickel in 0.1 M HCl solution in the absence and presence of 9 x 10^{-6} M concentration at temperature ranging from 30 to 60 °C was studied using polarization measurements.

Plot of logarithm of corrosion rate (log k), with reciprocal of absolute temperature (1/T) for Ni in 0.1 M HCl at 9 x 10^{-6} M for the investigated sulfa guanidine azomethine derivatives is shown in Figure (8). As shown from this Figure, straight lines with slope of -Ea*/ 2.303R and intercept of A were obtained according to Arrhenius-type equation:

$$K = A \exp(-Ea^*/RT) \quad (9)$$

Where k is the corrosion rate, A is a constant depends on a metal type and electrolyte, Ea* is the apparent activation energy, R is the universal gas constant and T is the absolute temperature.

Plot of log (corrosion rate/ T) vs. 1/ T for Ni in 0.1 M HCl at 6 x10^{-4} M for the investigated sulfa guanidine azomethine derivatives is shown in Figure (9). As shown from this Figure, straight lines with slope of (-ΔH*/ 2.303R) and intercept of (log R/ Nh + ΔS*/2.303R) were obtained according to transition state equation:

$$\text{Rate} = RT/Nh \exp(\Delta S^*/R) \exp(-\Delta H^*/RT) \quad (10)$$

Where h is Planck's constant, N is Avogadro's number, ΔH* is the activation enthalpy and ΔS* is the activation entropy. The calculated values of the apparent activation energy, Ea*, activation enthalpies, ΔH* and activation entropies, ΔS* are given in Table (8). The linear regression coefficients (R2) are close to unity, indicating that the corrosion of nickel in 0.1 M HCl solution may be elucidated using the kinetic model. These values indicate that the presence of the additives increases the activation energy, Ea* and the activation enthalpy, ΔH* and decreases the activation entropy, ΔS* for the corrosion process. The higher values of, Ea*, suggest that dissolution of nickel is slow in presence of inhibitors. It is clear that the higher values of Ea* lead to the lower corrosion rate. Also, the increase in the, Ea*, indicates strong adsorption of the inhibitor molecules on Ni surface and the presence of energy barrier caused by the adsorption of the additive molecules on Ni surface. The increase in the activation enthalpy (ΔH*) in the presence of the inhibitors implies that the addition of the inhibitors to the acid solution increases the height of the energy barrier of the corrosion reaction to an extent depends on the type and concentration of the present inhibitor. The positive sign of (ΔH*) indicates the endothermic behavior of these inhibitors at activated states. The entropy of activation (ΔS*) in the blank and inhibited solutions is large and negative indicating that the activated complex represents association rather than dissociation step [69, 70]. The order of decreasing inhibition efficiency, as observed from the increase in activation energy, is as follows: Compound (B) > Compound (A).

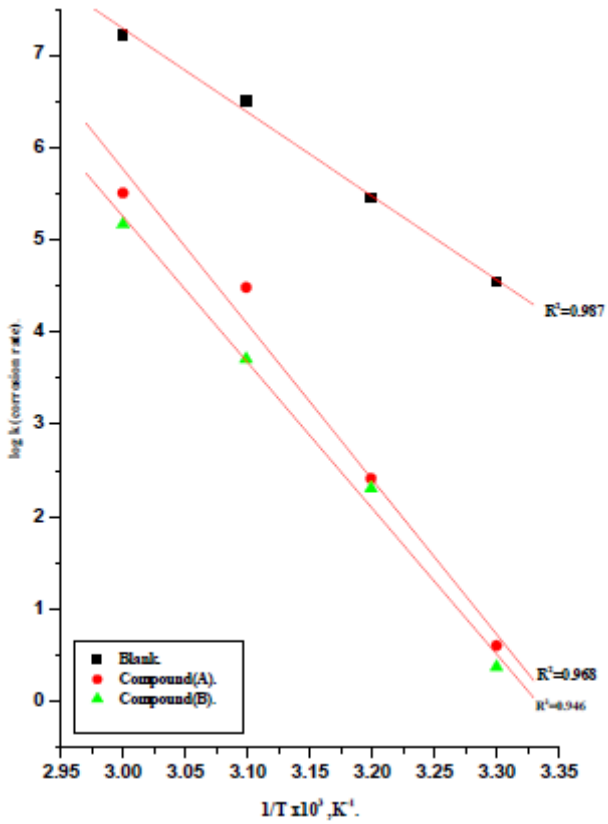

FIGURE (8): LOG CORROSION RATE VS. 1/T CURVES FOR THE CORROSION OF NICKEL IN 0.1 M HCL AT 9 X 10^{-6} M FOR INVESTIGATED SULFA GUANIDINE AZOMETHINE DERIVATIVES.

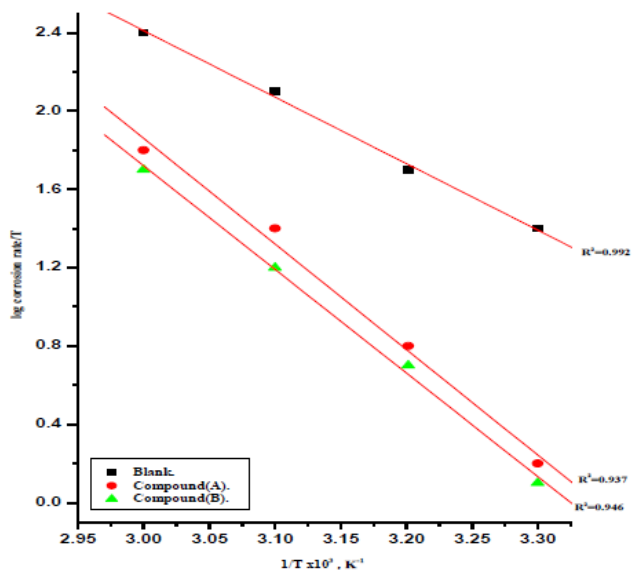

FIGURE (9): LOG CORROSION RATE/T VS. 1/T CURVES FOR THE CORROSION OF NICKEL IN 0.1 M HCL AT 9 X 10^{-6} M FOR INVESTIGATED SULFA GUANIDINE AZOMETHINE DERIVATIVES.

TABLE (8): KINETIC PARAMETERS FOR THE DISSOLUTION OF NI IN THE PRESENCE AND ABSENCE OF 9 X 10^{-6} M OF THE INVESTIGATED SULFA GUANIDINE AZOMETHINE DERIVATIVES IN 0.1 M HCL.

Compounds	Activation Parameters		
	E^*_a, kJ mol^{-1}	ΔH^* kJ mol^{-1}	$-\Delta S^*$ J mol^{-1} k^{-1}
0.1 M HCl	18.1	6.7	178.0
(A)	33.5	10.7	154.2
(B)	36.3	11.3	144.9

4.6. Mechanism of corrosion inhibition

The essential effect of these sulfa guanidine azomethine compounds as corrosion inhibitors is due to the presence of free electron pairs in the nitrogen, oxygen and sulfur atoms, d π-electrons on the aromatic rings, molecular size, heat of hydrogenation, mode of interaction with the metal surface and formation of metallic complexes.

It is generally, assumed that adsorption of the inhibitor at the metal / solution interface is the:

i) First step in the action mechanism of the inhibitors in aggressive acid media. Four types of adsorption may take place during inhibition involving organic molecules at the metal / solution interface [71]:

Electrostatic attraction between charged molecules and charged metal

ii) Interaction of unshared electrons pairs in the molecule with the metal.

iii) Interaction of π electrons with the metal and

iv) A combination of the above.

Concerning inhibitors, the inhibition efficiency depends on several factors; such as: (a) the number of adsorption sites and their charge density, (b) molecular size, heat of hydrogenation, (c) mode of interaction with the metal surface, and (d) the formation metallic complexes [72].

Most organic inhibitors contain at least one polar group with an atom of nitrogen, sulfur or oxygen, each of them in principle representing an adsorption center. The inhibitive properties of such inhibitors depend on the electron densities surrounding the adsorption centers: the higher the electron density at the center, the more the effective the inhibitor. Also, it is apparent that the adsorption of these inhibitor molecules on the nickel surface could occur directly on the basis of donor-acceptor behavior between the lone pairs of the heteroatom and the extensively delocalized π-electrons of the inhibitor molecule and the vacant d-orbital of nickel surface atoms [73]. These inhibitors are able to absorb on anodic sites through N, O atoms, heterocyclic and aromatic rings which

are electron donating groups. The adsorption of these inhibitors on anodic sites may decrease anodic dissolution of nickel. In the aqueous acidic solutions, most of organic inhibitors containing N atoms exist either as neutral molecules or in the form of cations (protonated). In general two modes of adsorption could be considered. In our case, the neutral form is the preferable one, the inhibitor molecules may adsorb on the Ni surface via the chemisorption mechanism, involving the displacement of water molecules from the metal surface and the sharing electrons between the N, and O atoms and Ni. The order of increased inhibition efficiency for sulfa guanidine azomethine derivatives is: Compound (B) > Compound (A). as indicated from the different methods.

Compound (B) is the most efficient inhibitor. This is due to its larger molecular size and the presence of nine N atoms, five O atom and one S atom. Compound (A) comes after Compound (B) in the inhibition efficiency. This is due to the presence of four N atom, six O atom, one S atom and lower molecular size than Compound (B).

5. Conclusions

In this paper, Potentiodynamic Polarization, Electrochemical Impedance Spectroscopy (EIS) and density functional theory studies of sulfa guanidine azomethine as efficient corrosion inhibitors for nickel surface in hydrochloric acid solution. The principal conclusions are:

1) The inhibition efficiency of sulfa guanidine azomethine derivatives increases by increasing the inhibitor concentration, but it decreases with increase in temperature.

2) The bond gap energy ΔE increases from compound (B) to compound (A). This fact explains the decreasing inhibition efficiency in this order Compound (B) > Compound (A).

3) Ac impedance plots of nickel indicated that polarization resistance increases with increase in inhibitor concentration.

4) The negative sign of $\Delta G°_{ads}$ indicates that the adsorption process is spontaneous.

5) The increase in activation energy after the addition of inhibitors to the 0.1 M HCl solution indicates that the adsorption is more physical than chemical.

6. References

[1] H. G. Feller, H. G. Ratzer Scheibe, Electrochim. Acta, 17(1972)17.
[2] H. G. Feller, H. G. Ratzer Scheibe, W. Wendt, Electrochim. Acta, 18 (1973) 175.
[3] H. G. Feller, M. Kesten, J. Krupski, Proc. Int. Congr. Corros., 515 (1974) 155.
[4] H. G. Feller, M. Kesten, H. G. Ratzer Scheibe, Proc. 5th Int. Comgr. Metal Corrosion, 149(1974).
[5] M. C. Petit, A. Jouanneau, Proc. 5th Int. Comgr. Metal Corrosion, 237 (1974).
[6] I. Graz, B. Galzer, Corros. Sci., 14 (1974) 253.
[7] L. A. Barkalatsova, A. G. Pshenicknikov, Electrochem., 12 (1976) 42.
[8] N. A. Balashova, N. T. Gorokova, M. I. Kulesnova, S. A. Libin, D. C. Soobsch, 3 (1976) 264.
[9] M. Kesten, Corrosion, 32 (1976) 94.
[10] I. L. Soruskhim, G. A. Tedoradze, G. I. Kaurova, T. I. Raxmerova, Electrokhim., 12 (1976) 442.
[11] E. I. Mikhailova, Z. A. Iofa, Ind. J. Chem., 12 (1974) 664.
[12] H. Breushke, F. Weller, K. H. Ebert, Werk. U. Korros., 27 (1974) 664.
[13] A. M. Maitra, K. Bhattacharyya, J. Ind. Chem. Soc., LVI (1979) 1202.
[14] A. S. Fouda, A. Al-Sarawy and T. M. Omar, Annali di chim., 95 (2005) 53.
[15] A. S. Fouda, A. A. El-Shafei and H. E. Gadow, Port. Electrochim. Acta, 20 (2002) 13.
[16] A. S. Fouda, H. E. Gadow and A. A. El-Shafei, KorroziosFigyelo, 43 (3) (2003) 95.
[17] G. Schmit, Br. Corros. J., 19(4) (1984) 465.
[18] G. Lewis, Corros. Sci., 22 (1982) 579.
[19] S. Rengamani, I. Vasudvan and S. V. K. Lyer, IND. J. Technol.,31 (1993) 519.
[20] M. Stern and A. I. J. Geary, J. Electrochem. Soc.,104 (1957) 56.
[21] A. K. Maayta and N. A. F. Rawshdeh, Corros.Sci., 46 (2004) 1129.
[22] A. A. Aksut, S. Bilgic, Corros. Sci., 33 (1992) 379.
[23] E. Khamis, F. Bellucci, R.M. Latanision, E.S.H. El-Ashry, Corrosion, 47 (1991) 677.
[24] S.M. Reshetnikov, Port. Met., 14 (1978) 491.
[25] V. Sastry, R. Packwood, Werkst. Korros., 38 (1987) 77.
[26] A. Frignani, C. Monticelli, G. Trabanelli, Br. Corros. J., 33 (1998) 71.
[27] C. F. Zinola, A. H. Castro Luna, Corros. Sci., 37 (1995) 1919.
[28] K. Bajpai, G. Singh, Bull. Electrochem., 16 (2000) 241.
[29] A. S. Fouda, G. Y. Elewady and K. Shalabi, Mansoura J. Chem., 35(2) (2008) 35.
[30] T.Tsuru, S. Haruyama and G. Boshku, J. Jpn. Soc. Corros. Eng. 27 (1978) 573.
[31] M. Abdallah, S. O. Alkaranee, A. A. Abdel Fattah, ZSastita Materijala, 50 (2009) 205-212.
[32] G. Y. Elewady, A. El-Askalany, A. F. Molok, Port. Electrochim. Acta, 26 (6) (2008) 503-516.
[33] M. Abdallah, A.Y.El-Etre, Port. Electrochim. Acta, 21 (2003) 315-326.
[34] S. Hinnov, J. Tamm, Chemistry, 60 (3) (2011)184-192.
[35] M. Walia, G. Singh, Surf. Eng., 21 (3) (2005) 176-179.
[36] I. Sheikhshoaie, M. Hossein, Mashhadizadeh, and S. Saeid-Nia, J. Coordination Chemistry. 57(5) (2004) 417.
[37] Gaussian 98, Revision A.6, M. J. Frisch, G. W. Trucks, H. B. Schlegel, G. E. Scuseria, M. A. Robb, J. R. Cheeseman, V.G. Zakrzewski, J.A. Montgomery, Jr.,R.E.Stratman J.C.Burant, S.Dapprich, J.M.Millam, A.D.Daniels, K.N. Kudin, M.C. Strain, O. Farkas, J. Tomasi, V. Barone, M. Cossi, R. Cammi, B.Mennucci, C. Pomelli, C. Adamo, S.Clifford, J. Ochterski, G. A. Petersson, P. Y. Ayala, Q. Cui, K. Morokuma, D. K.Malick, A.D.Rabuck, K. Raghavachari, J.B. Foresman, J.Cioslowski, J.V.Ortiz, B.B.Stefanov, G.Liu, A.Liashenko, P.Piskorz, I. Komaromi, R.Gomperts,R. L. Martin, D. J. Fox, T. Keith, M. A. Al-Laham, C. Y. Peng, A. Nanayakkara, C. Gonzalez, M. Challacombe, P. M. W. Gill, B. Johnson, W. Chen, M. W. Wong, J. L.Andres, C. Gonzalez, M. Head-Gordon, E. S. Replogle, and J. A. Pople, Gaussian, Inc., Pittsburgh PA, (1998) .
[38] W. J. Stevens, M. Krauss, H. Bosch and P. G. Jasien, Can. J. Chem. 70 (1992)612.
[39] E. S. Ferreira, C. Giancomlli, F. C. Giancomlli and A. Spinelli, Mater. Chem. Phys., 83 (2004) 129.
[40] W. Kohn, L. J. Sham, Phys. Rev A 140(1965)1133.

[41] A. D. Becke, Phys. Rev. A 38(1988)3098.
[42] C. Lee, W. Yang, R. G. Parr, Phys. Rev B (1988)37.
[43] R. L. Flurry Jr., Molecular Orbital Theory of Bonding in Organic Molecules, Marcel Dekker, New York, 1968.
[44] I. Turel, L. Golic, P. Bukovec and M. Gubina, Journal of Inorganic Biochemistry 71(1998)53.
[45] I. Turel, P. Bukovec, M. Quiros, Int. J. Pharm. 152 (1997) 59.
[46] Yue Yang, Hongwei Gao, Spectrochemica Acta part A 85(2012) 303-309
[47] S. Sagdinc and S. Bayari, Journal of Molecular Structure 691 (2004) 107-113
[48] A. Yoshida, R. Moroi, Anal. Sci. 7(1991)351.
[49] S. Sagdinc and S. Bayari, Journal of Molecular Structure (THEOCHEM) 668 (2004) 93-99.
[50] I. Fleming Frontier Orbitals and Organic Chemical Reactions, Wiley, London, 1976.
[51] A. S. Fouda, H. M. El-Abbasy, Corrosion (NACE) 68(1)(2012) 1-9.
[52] L. J. Vracar and D. M. Drazic, Corros. Sci., 44 (2002) 1669
[53] X. H. Liand S. D. Deng, Corros. Sci., 509 (2008) 420.
[54] T. Paskossy, J. Electroanal. Chem., 364 (1994) 111
[55] J. Bessone, C. Mayer, K. Tuttner and W. Lorenz, J. Electrochim. Acta., 28 (1983) 171
[56] A. Caprani, I. Epelboin, Ph. Morel and H. Takenouti, Proceedings of th 4th European Sym. On Corrosion Inhibitors, Ferrara, Italy, 571(1975).
[57] I. Epelboin, M. Keddam and H. Takenouti, J. Appl. Electrochem., 27 (1972) 1.
[58] E. McMCafferty, N. Hackerman, J. Electrochem. Soc., 119(1972) 146.
[59] S.Muralidharan, K. L. N. Phani, S. Pitchumani, S. Ravichandran, J. Electrochem. Soc., 42 (1995) 1478.
[60] A.Asan, ,M.Kabasakaloglu, M.Isiklan and Z.Kilic, Corros.Sci., 47 (2005) 1534.
[61] A. S. Fouda, M. Abdallah and R. A. El-Dahab, Desalination and Water Treatment, 22(2) (2010) 340
[62] A. S. Fouda, S. T. Shawagfeh, Bull. Soc. Chim. Fr., 127 (1990) 30.
[63] S. I. Da Costa, and S. M. L. Agostinho, J. Electroanal. Chem., 196(1) (1990) 51.
[64] L. Tang, X. Li, L. Lin, G. Mu, and G. Liu, Mater. Chem. Phys., 97 (2006) 301.
[65] K. Tebbji, N. Faska, A. Tounsi, H. Ouddad, M. Benkaddour and B. Hammouti, Mater. Chem.Phys., 106 (2007) 2144.
[66] G. Mu, X. Li, and G. Liu, Corros. Sci., 47 (2005) 1932.
[67] S. A. Ali, H. A. Al-Muallem, M. T. Saeed and S.U.Rahman, Corros. Sci., 50 (2008) 664.
[68] E. A. Noor, and A. H. Al-Moubaraki, Corros. Sci., 51 (2009) 868.
[69] G. K. Gomma and M. H. Wahdan, Mater. Chem. Phys., 30 (1995) 209
[70] M. S. Soliman and Ph. D. Thesis, Alex. Univ., Egypt (1995).
[71] D. Schweinsberg, G. George, A. Nanayakkara and D. Steiner, Corros. Sci., 28 (1988) 55.
[72] A. S. Fouda, M. N. Mousa, F. I. Taha and A. I. Elneanaa, Corros. Sci., 26 (1986) 719.
[73] S. Muralidharan, M. A. Quraishi, and SV. K. Iyer, Corros. Sci., 37 (1995) 1739.